Reaction $^{42}Ca(p, t)^{40}Ca$ and the structure of ^{40}Ca†

P. T. Debevec* and G. T. Garvey
Joseph Henry Laboratories, Princeton University, Princeton, New Jersey 08540
(Received 27 March 1974)

The reaction $^{42}Ca(p, t)^{40}Ca$ was studied at 41.7 MeV; angular distributions were obtained over the range from 10 to 60°. The lowest $T = 1$, 0^+ state was identified at 9.386 ± 0.012 MeV by comparison with the analog reaction $^{42}Ca(p, {}^3He)^{40}K(1.639\ MeV)$. The weak population of these states is attributed to destructive interference between $d_{3/2}{}^2$ pickup from the two-particle component of ^{42}Ca and $f_{7/2}{}^2$ pickup from the four-particle two-hole component of ^{42}Ca. The excitation energy of these states cannot be accounted for by the $f_{7/2}$-$d_{3/2}$ effective interaction. Spectroscopic amplitudes for the Gerace-Green wave functions are calculated in a shell-model basis. Distorted-wave Born-approximation (DWBA) calculations for the lowest $T = 0$ and $T = 1$, 3^-, and 5^- states are in qualitative agreement with the data. The DWBA calculations for the positive-parity states show greater pickup strength to the two-particle two-hole 0^+ and 2^+ states than to the four-particle four-hole 0^+ and 2^+ states. The experimental results are the opposite: the four-particle four-hole states are populated more strongly than the two-particle two-hole states. Although there are uncertainties in the DWBA calculations, it is suggested that the inability to account for the observed two-nucleon pickup demonstrates a deficiency in the Gerace-Green model.

[NUCLEAR REACTIONS $^{42}Ca(p,t)$, $E = 41.7$ MeV; measured $\sigma(E_t, \theta)$. ^{40}Ca deduced levels, J, π, l. Enriched target.]

INTRODUCTION

The elucidation of the structure of ^{40}Ca has been the focus of a considerable experimental and theoretical effort. In a comprehensive discussion of the electromagnetic transitions, MacDonald, Wilkinson, and Alburger[1] have demonstrated that the model of Gerace and Green[2-4] is highly successful in accounting for the electromagnetic widths of the low-lying spectrum. Similarly, Goode[5] has compared several calculations of the electromagnetic widths of the negative-parity states and found that only the model of Gerace and Green could account for the data. The picture then of deformed multiparticle-multihole states coexisting with spherical shell-model states is central to our current understanding of the structure of ^{40}Ca.

Although single-nucleon transfer experiments are largely in agreement with the model of Gerace and Green, they are relatively insensitive to the presence of multiparticle-multihole components. We have obtained data for the two-nucleon transfer reaction $^{42}Ca(p, t)^{40}Ca$, which is sensitive to these components, and we have analyzed these data in the framework of the conventional two-nucleon transfer theory. This reaction has been studied previously,[6-8] and our results, obtained at high bombarding energy with good energy resolution, complement and extend previous work. Brief accounts of our work have already appeared, wherein we discussed the failure of the coexistence model to account for the observed strength to the $T=0$, 0^+ states,[9] and the anomolous yield to the $T=1$, 0^+ state.[10] Herein we amplify on these remarks and discuss several other points.

EXPERIMENTAL METHOD

A 41.7-MeV proton beam from the Princeton A.V.F. cyclotron was used to bombard isotopically enriched ^{42}Ca that was evaporated onto a thin organic backing and transferred *in vacuo* to a 60-in. scattering chamber. Silicon surface-barrier detectors were used in the ΔE-E configuration to provide signals for particle identification and energy analysis. The pulse-processing electronics included veto and pileup rejection circuitry. Particle identification was accomplished by the stored range-energy look-up table method, and the particle-sorted spectra were stored in a XDS Σ2 computer to be written later on magnetic tape.

Considerable care was exercised in obtaining good energy resolution and low background. Contributions to the resolution from beam energy spread, beam-spot size, detector aperture, and target thickness were equalized so that a line width of 32 keV was obtained for tritons. High counting rates (10–20 kHz) were permitted by the pileup rejection performed on fast signals from Sherman-Roddick preamplifiers.[11] A spectrum ob-

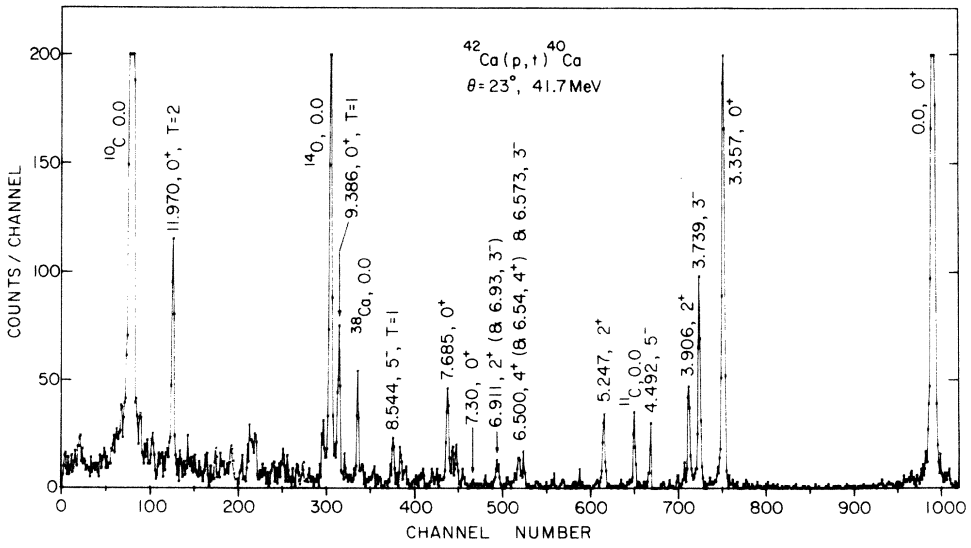

FIG. 1. Spectrum of $^{42}Ca(p,t)^{40}Ca$ obtained at 23°, the second maximum of $L=0$ transfer. Energy resolution is 32 keV.

tained at 22° (the second maximum of $L=0$ transfer) is shown in Fig. 1.

Excitation energies were obtained with the program "QPLOT" and yields were extracted with the spectrum analysis program "AUTOFIT."[12] Relative normalization of different angles was provided by a counter fixed at 90° monitoring elastics. The target thickness was roughly determined by comparing the width of triton and ^3He lines to provide an absolute cross section. Within the accuracy of this method, this normalization agrees with more precise determinations of the absolute cross section.[8]

EXPERIMENTAL RESULTS

A summary of states identified in the ^{40}Ca spectrum is given in Table I. Comparison to energies from previous work demonstrates that the assignments are, in most cases, unambiguous. Spin and parity assignments are from previous work and are listed for reference.

A. Identification of the $T=1$, 0^+ state

The state at 9.386 MeV can be unambiguously identified as the lowest $T=1$, 0^+ state. The excitation energy is in good agreement for the expected analog of the 1.639-MeV ^{40}K, 0^+, $T=1$ state,[13] and the angular distribution displays the characteristic $L=0$ shape. The angular distributions for the ^{40}Ca $T=1$ and $T=2$, 0^+ states, and the ^{40}K $T=1$ and $T=2$, 0^+ states are given in Figs. 2 and 3. Contrary to the expectation based on a model of these states as two-particle two-hole,[14] the $T=1$ states are considerably weaker than the $T=2$ states. The ratios of the maximum cross section (observed at approximately 22°) of the $T=1$ states to the $T=2$ states are 0.65 ± 0.05 for ^{40}Ca and 0.10 ± 0.01 for ^{40}K.

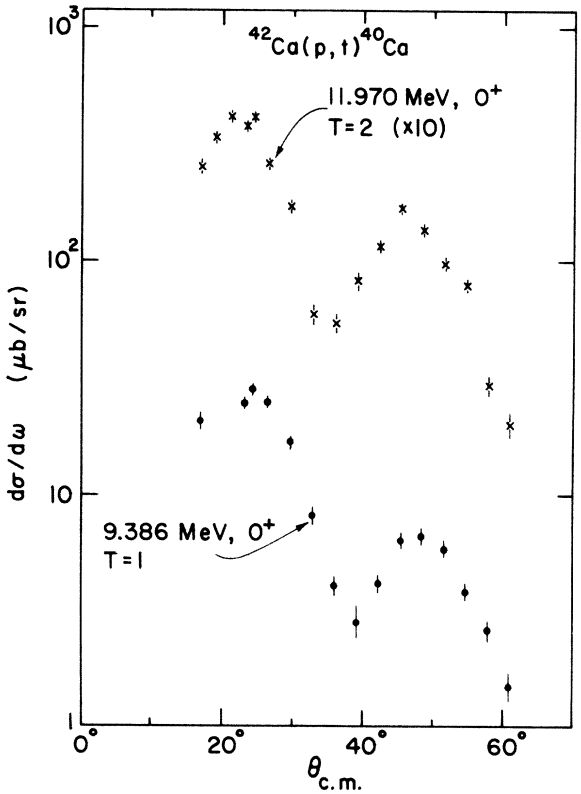

FIG. 2. Angular distributions of $^{42}Ca(p,t)^{40}Ca$ $T=2$ and $T=1$, 0^+ states. At 20° the $T=1$ state was obscured by the oxygen contaminent.

TABLE I. Observed excitation energies in ^{40}Ca.

Energy (MeV)	Error (keV)	Previous work	Spin	Parity	Strength [a]
g.s.		g.s.	0	+	412. (7.4) at 20°
3.357	7	3.353	0	+	96.0 (3.6) at 20°
3.739	7	3.737	3	−	38.9 (2.3) at 20°
3.906	8	3.904	2	+	35.0 (3.0) at 14°
4.492	7	4.492	5	−	18.1 (1.5) at 20°
5.247 [b]	10	5.249	2	+	
5.617	6	5.628	2	+	Weak
5.90		5.903	1	−	Very weak
6.03		6.025	2	−	Very weak
		6.029	3	+	
6.498 [c]	10	6.509	4	+	
6.573	10	6.579	3	−	
6.75		6.752	2	−	Very weak
6.911 [d]	11	6.910	2	+	8.4 (1.0) at 18°
7.105	8	7.114	(2)	(+)	
		7.117	(3)	(−)	
7.285	16	7.28	?	?	2.3 (0.6) at 18°
		7.30	0	?	
7.40		7.399	6	+	Very weak
7.453	9	7.455	?	?	Weak
7.550	9	7.558	4	+	
7.619	15	7.620	?	?	
7.685 [e]	12		0	+	19.7 (2.3) at 18°
7.850	12	7.867	2	+	Weak
7.919	15	7.928	2	+	Weak
8.079	10	8.092	2	+	Weak
8.181	15	8.186	2	+	Weak
8.34		8.321	?	?	Very weak
8.418	10	8.424	?	?	Weak
8.544($T=1$)	11	8.543	5	−	12.2 (1.2) at 16°
9.386($T=1$) [e]	13		0	+	28.0 (1.7) at 23°
9.629($T=?$)	15				
11.970($T=2$)	12	11.978	0	+	41.2 (2.3) at 20°

[a] If listed, the strength is given at the laboratory angle of the measured maximum cross section with its error in μb/sr. "Weak" and "very weak" are, respectively, of the order of a few μb/sr and less than 1 μb/sr.

[b] Triplet at 5.212 (0^+), 5.249 (2^+), 5.279 (4^+).

[c] Doublet at 6.509 (4^+) and 6.541 (4^+).

[d] Triplet at 6.910 (2^+), 6.930 (3^-), and 6.951 (1^-).

[e] Spin and parity assignment from this experiment.

B. Excitation of the positive-parity states

Two of the previously identified $T=0$, 0^+ states were observed. The angular distributions of the ground state and the 3.357-MeV state are presented in Fig. 4. In the calculation of Gerace and Green these states have been taken to be predominantly zero-particle zero-hole and four-particle four-hole, respectively. The two-particle two-hole 0^+ state has not been previously identified. The suggested candidate at 7.30 MeV[15] is found to be very weakly excited, and the measured excitation energy of the observed state, 7.285 MeV, is also consistent with a state of unknown spin. Also presented in Fig. 4 is the angular distribution of a 7.685-MeV state. The angular distribution suggests a 0^+ assignment,[16] and the excitation energy is not inconsistent with that required by Gerace and Green. This state then is taken to be the two-particle two-hole $T=0$, 0^+ state, although some strength appears higher in excitation.[16] The ratio of cross sections integrated over the angular range observed of the zero-particle zero-hole, the four-particle four-hole, and the two-particle two-hole states is 100 : 20.6 : 4.8.

There was no evidence of excitation of the known 0^+ state at 5.201 MeV. The angular distribution of the state which was excited (Fig. 5) does not have maxima appropriate to an $L=0$ angular distribution. Its measured excitation energy, 5.247

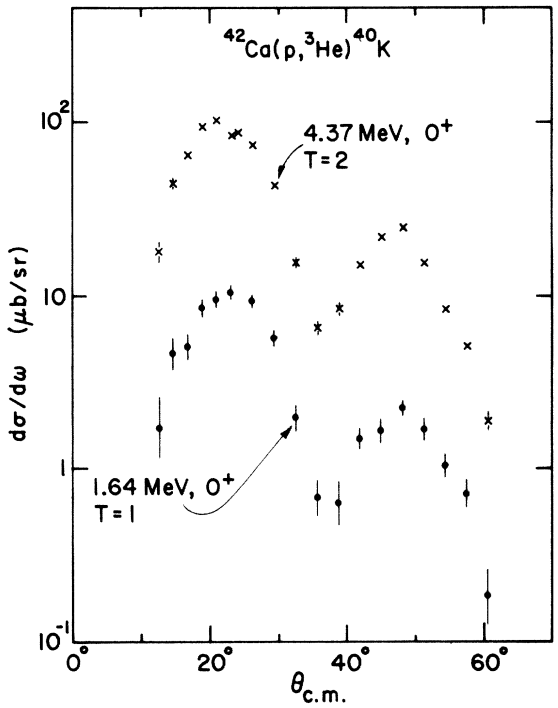

FIG. 3. Angular distributions of $^{42}Ca(p,^3He)^{40}K$ $T=2$ and $T=1$, 0^+ states.

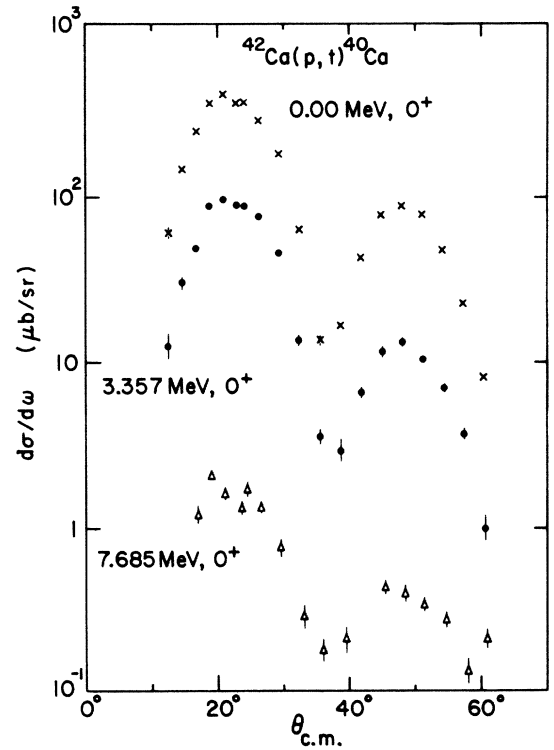

FIG. 4. Angular distributions of $^{42}Ca(p,t)^{40}Ca$ $T=0$, 0^+ states.

MeV, is consistent with the known 2^+ state. The nonobservation of this state is consistent either with the speculation that it is eight-particle eight-hole[4] or that it is four-particle four-hole with the particles and holes each coupled to $T=2$.[17] In the region of 7–9 MeV several other lines were identified (7.453, 7.551, 7.619, 8.418, and 9.629 MeV). These states had rather characterless angular distributions but were manifestly not $L=0$ patterns. Therefore, no other $T=0$, 0^+ states of any appreciable strength have been identified.

Several known 2^+ states were observed. In the calculation of Gerace and Green, the band members of the four-particle four-hole and two-particle two-hole 0^+ states are taken to be the 2^+ states at 3.904 and 6.910 MeV. The higher state is a member of a triplet (2^+ at 6.910 MeV, 3^- at 6.930 MeV, and 1^- at 6.958 MeV) which could not be resolved in the present experiment. Even so, the measured excitation energy of the state observed, 6.911 MeV, favors identification with the 2^+ state. The 6.911-MeV state is excited approximately one-third as strong as the 3.907-MeV state. This relative cross section, and the relative cross section to the 0^+ states are discussed below. The other states which are identified with known 2^+ states (5.617, 7.103, 7.850, 7.919, 8.089, and 8.181 MeV) are all weak, and they have rather characterless angular distributions. No identification of their spin and parity could be made on the basis of their angular distributions, but this uncertainty may be due to poor statistics.

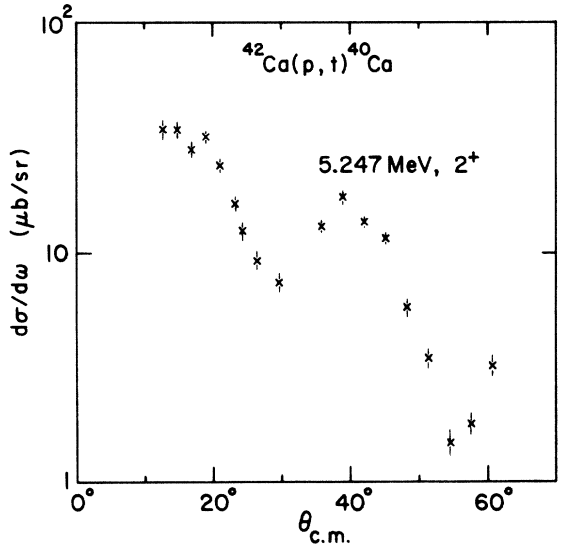

FIG. 5. Angular distribution of $^{42}Ca(p,t)^{40}Ca$ 5.247-MeV 2^+ state. The minima and maxima are shifted with respect to an $L=0$ transfer showing no evidence of the 5.201-MeV 0^+ state.

C. Excitation of the negative-parity states

The lowest $T=0$, 3^-, and 5^- states were identified with the states observed at 3.739 and 4.492 MeV, respectively. The yield associated with the 8.544-MeV excitation was identified with the lowest $T=1$, 5^- state. The 5^- states have similar angular distributions and approximately equal cross sections. The $T=1$, 3^- state at 7.693 MeV would not be resolved from the 7.685-MeV (0^+) state, and on the basis of sound theoretical considerations, its cross section is expected to be very small. As the minimum observed at 37° in the angular distribution of the 7.685-MeV state is quite distinct, the yield to the $T=1$, 3^- state must be small. No other known negative-parity state has any appreciable strength.

Lastly, it should be mentioned that the natural parity selection rule in the conventional two-nucleon transfer theory is well satisfied. The easily resolved unnatural parity states at 6.030 and 6.752 MeV are no stronger than 0.5 μb/sr at any angle.

TWO-NUCLEON TRANSFER THEORY

A concise exposition of two-nucleon transfer theory, applicable to shell-model basis states, has been given by Towner and Hardy.[18] Their expression for the cross section (their 2.49) for the reaction $A+a \rightarrow B+b$ is

$$\frac{d\sigma}{d\Omega}=\frac{\mu_a\mu_b}{(2\pi\hbar^2)^2}\frac{k_b}{k_a}\frac{2S_b+1}{2S_a+1}\sum_{M\sigma_a\sigma_b}^{J}\left|\sum_{\substack{[n_1l_1i_1][n_2l_2i_2]\\LST}} b_{ST}S_{AB}{}^{1/2}([n_1l_1j_1][n_2l_2j_2]JT)(T_BN_BTN\,|\,T_AN_A)\begin{bmatrix} l_1 & l_2 & L\\ \frac{1}{2} & \frac{1}{2} & S\\ j_1 & j_2 & J\end{bmatrix}B^{LSJT}_{M\sigma_a\sigma_b}\right|^2 .$$

The spectroscopic amplitude,

$$S_{AB}{}^{1/2}([n_1l_1j_1][n_2l_2j_2]JT),$$

is essentially a two-particle fractional-parentage coefficient. The summation over the two-particle configurations, $([n_1l_1j_1][n_2l_2j_2])^{JT}$, which can connect the initial and final states is coherent. Because of this coherent summation over these spectroscopic amplitudes, the calculation of two-nucleon transfer reactions is most sensitive to the wave functions assumed for the initial and final states. Although this coherence makes it virtually impossible to extract wave functions from an analysis of the experimental data, it makes it possible to test wave functions produced by structure calculations.

The salient feature in the calculation of $B^{LSJT}_{M\sigma_a\sigma_b}$ (in the local, zero-range approximation) is the assumption that the interaction occurs between the incoming particle and the center of mass of the transferred pair. This assumption has two consequences. The relative motion of the transferred pair cannot change, and the center of mass of the pair serves as the form factor. Since the particles in the triton or ^{3}He are in relative S states, it is the relative angular-momentum zero component of the two-particle configuration (j_1j_2) which determines the contribution to the cross section. For example, transfer of $p_{3/2}{}^2$ is favored over transfer of $f_{7/2}{}^2$. Since $(1f2p)$ particles have more energy than $(2s1d)$ particles, the center-of-mass coordinate of an (fp) pair oscillates more than that of an (sd) pair. For $L=0$, $(fp)^2$ has three nodes, while $(sd)^2$ has two nodes (see Fig. 11). This latter consideration proves to be important in the superposition of $(1f2p)^2$ configurations and $(2s1d)^2$ configurations.

Some estimate of the accuracy of the transfer theory (in the local, zero-range approximation) can be gleaned from the analysis of ^{208}Pb$(p, t)^{206}$Pb by Glendenning[19] and the analysis of $1p$-shell transitions by Kahana and Kurath.[20] These analyses can serve as an indication of the accuracy of the transfer theory as the wave functions are well established. It appears from these analyses that, given an arbitrary normalization between the experiment and the calculation, all transitions can be calculated to within a factor of 2. Hence, if the nuclear structure has been well described, and the standard procedures of the calculation respected, relative cross sections should be predicted to within a factor of 2.

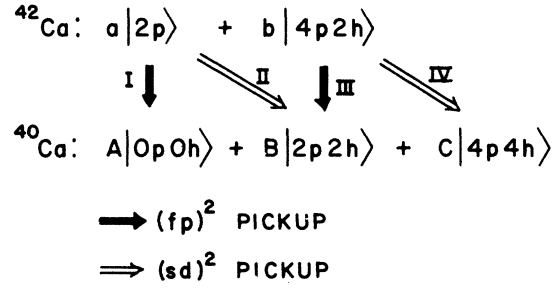

FIG. 6. Transition amplitudes connecting ^{42}Ca and $T=0$ positive-parity states of ^{40}Ca.

CALCULATION OF THE SPECTROSCOPIC AMPLITUDES

As the wave functions of Gerace and Green are in a Nilsson model basis, a projection into a spherical basis must be performed to calculate the spectroscopic amplitudes. We have constructed the deformed states, projected into a spherical basis, and calculated the overlap of the initial and final states. For example, the spherical expansion of a $K=0$ two-particle deformed state is

$$|2p\ K=0JM\rangle = n_J \sum_{j_1\geq j_2} \frac{1}{(1+\delta_{j_1 j_2})^{1/2}} (j_1\tfrac{1}{2} j_2 -\tfrac{1}{2}\,|\,J0)\,\chi(j_1\tfrac{1}{2})\chi(j_2-\tfrac{1}{2})\,|\,(j_1 j_2)JM\rangle$$

$$\equiv n_J \sum_{j_1\geq j_2} V(j_1 j_2 J)\,|\,(j_1 j_2)^J\rangle\,,$$

where $\chi(j\frac{1}{2})$ is an expansion coefficient for Nilsson orbital No. 14, n_J normalizes the wave function, and $V(j_1 j_2 J)$ is introduced to compress the notation. With a similar expression for the spherical expansion of a two-hole state using Nilsson orbital No. 8, we constructed the spherical expansion of the two-particle two-hole state by coupling the two. Our expression for the two-particle two-hole state is

$$|\,2\text{p2h}\ K=0JM\rangle = m_J \sum_{j_1\geq j_2}\sum_{j_3\geq j_4}\sum_{J_p J_h} \frac{1}{(1+\delta_{j_1 j_2})^{1/2}}\frac{1}{(1+\delta_{j_3 j_4})^{1/2}} (j_1\tfrac{1}{2} j_2 -\tfrac{1}{2}\,|\,J_p 0)(j_3\tfrac{3}{2} j_4 -\tfrac{3}{2}\,|\,J_h 0)$$

$$\times (J_p 0 J_h 0\,|\,J0)\chi(j_1\tfrac{1}{2})\chi(j_2-\tfrac{1}{2})\chi(j_3\tfrac{3}{2})\chi(j_4-\tfrac{3}{2})\,|\,[(j_1 j_2)^{J_p}(j_3^{-1} j_4^{-1})^{J_h}]JM\rangle$$

$$\equiv m_J \sum_{\substack{j_1 j_2 j_3 j_4 \\ J_p J_h}} X(j_1 j_2 j_3 j_4 J_p J_h J)\,|\,[(j_1 j_2)^{J_p}(j_3^{-1} j_4^{-1})^{J_h}]JM\rangle\,,$$

where m_J normalizes the wave function and $X(j_1 j_2 j_3 j_4 J_p J_h J)$ is introduced to compress the notation. From the expression Gerace and Green[2] give for the matrix element $\langle 2\text{p2h}\,|\,V\,|\,0\text{p0h}\rangle$, we could verify that our construction technique was correct. The construction of the other multiparticle-multihole states was analogous. The relevant expansions are given in the Appendix.

The four routes between the ^{42}Ca ground state and a positive-parity state in ^{40}Ca are indicated in Fig. 6. The method of obtaining these transitions is well illustrated by the calculation of the two-particle to two-particle two-hole transition. The two-particle state is written

$$|\,2\text{p}\rangle = \sum_{j_1} b_{j_1}\,|\,j_1^{\,2} J=0\rangle\,.$$

If $\theta^{[j_A j_B]J}$ is an operator which transfers the pair $(j_A j_B)^J$, the expression for the overlap, $\langle (2\text{p2h})J_f\,|\,\theta^{[j_A j_B]J}\,|\,(2\text{p})J_i=0\rangle$ is

$$\sum_{j_A\geq j_B}\sum_{j_1\geq j_2}\sum_{j_3\geq j_4}\sum_{j_5\geq j_6}\sum_{J_p J_h}\frac{1}{\sqrt{3}} b_{j_1 j_2} m_J X(j_3 j_4 j_5 j_6 J_p J_h J_f)\,\langle [(j_3 j_4)^{J_p}(j_5^{-1} j_6^{-1})^{J_h}]J_f\,|\,\theta^{[j_A j_B]J}\,|\,(j_1 j_2)J_i=0\rangle$$

$$= \sum_{j_3\geq j_4}\sum_{j_5\geq j_6}\frac{1}{\sqrt{3}} b_{j_3 j_4} m_{J_f} X(j_3 j_4 j_5 j_6 J_p=0\, J_h=J_f J_f)\,\langle \text{def}\,|\,\text{sph}\rangle F^{j_5 j_6 J_f}(R)\,.$$

The factor of $1/\sqrt{3}$ represents the neutron-particle neutron-hole part of the deformed state. The form factor $F^{j_5 j_6 J_f}(R)$ is calculated by the method of Bayman and Kallio[21] in the distorted-wave Born-approximation (DWBA) code DWUCK2,[22] for which the remainder of the expression is a coefficient that is explicitly evaluated. Expressions for the three other routes connecting the ^{42}Ca ground state to a

positive-parity state in ^{40}Ca are given in the Appendix.

For the negative-parity states we neglected the possibility of deformed states as the four states of interest, the lowest $T=0$ and $T=1$, 3^- and 5^- states, are predominantly particle-hole states. Following Gerace and Green, Kuo's[23] wave functions were used for the negative-parity states and the ^{42}Ca ground state. The overlap between the ^{42}Ca ground state and a negative-parity state in ^{40}Ca is

$$\sum_{j_A \geq j_B} \sum_{j_p j'_p j_h} \frac{1}{\sqrt{2}} c_{j_p} d_{j_h j_p} \langle (j_h^{-1} j_p) J_f \mid \theta^{[j_A j_B] J} \mid (j_p^2) J=0 \rangle$$

$$= \sum_{j_h j_p} c_{j_p} d_{j_h j_p} \frac{1}{(2_{j_p}+1)^{1/2}} F^{j_h j_p j_f}(R),$$

where the c_{j_p} represent the two-particle amplitudes in the ^{42}Ca ground state, and the $d_{j_h j_p}$ represent the particle-hole amplitudes in the ^{40}Ca negative-parity states.

WAVE FUNCTION AND ENERGY OF THE $T=1, 0^+$ STATE

In both the (p, t) and $(p, {}^3\mathrm{He})$ the $T=1$, 0^+ state is much weaker than the $T=2$, 0^+ state. Damgaard has suggested that this suppression of the $T=1$ state relative to the $T=2$ state can be attributed to the presence of the four-particle two-hole component in the ^{42}Ca ground state. For the $T=2$ states the (fp) particle pickup and the (sd) particle pickup interfere constructively, but for the $T=1$ states these two routes interfere destructively. These two routes are shown in Fig. 7. Of course, it could also be the case that the $T=2$ and $T=1$ states

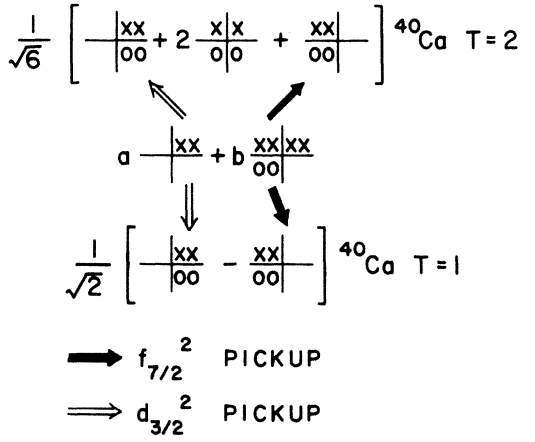

FIG. 7. Transition amplitudes connecting ^{42}Ca and the two-particle two-hole $T=2$ and $T=1$, 0^+ states. Note the change between the $T=2$ and $T=1$ state in the interference of $f_{7/2}{}^2$ pickup and $d_{3/2}{}^2$ pickup.

are not configuration states, but a simple diagonalization of the $(f_{7/2}{}^2 d_{3/2}{}^{-2})$ basis shows that both states are overwhelmingly $(f_{7/2}{}^{2\ J=0} d_{3/2}{}^{-2\ J=0})$. This diagonalization is instructive as it demonstrates a peculiarity in the spectrum of the two-particle two-hole states.

The expressions required for a diagonalization in this space are given by de-Shalit and Talmi,[24] their (37.2) and (37.19). With matrix elements and particle-hole splitting obtained phenomenologically,[25] the lowest $T=2$, $T=1$, and $T=0$ states appear at 11.63, 6.72, and 3.27 MeV, respectively. Although the $T=2$ state is close to the experimental value, the $T=1$ state is low by 2.6 MeV, and the $T=0$ state appears close to the "known" four-particle four-hole state. The difficulty with respect to the $T=1$ state has been noted by Erné,[25] and in complete $(f_{7/2}{}^n d_{3/2}{}^{-n})$ space, Zucker[26] has obtained a similar result. Schapira *et al.*[8] correctly attribute this difficulty to the symmetry energy, which following Bansal-French[27] and Zamick[28,29] places the $T=1$ state 2×2.9 MeV from the $T=2$ state. What also should be noted is that the $T=0$ two-particle two-hole state appears very low in the spectrum. In fact this scheme would predict that the $T=0$, two-particle two-hole 0^+ state occurs 3×2.9 MeV below the $T=2$ state which would place it at 3.3 MeV. This energy is in excellent agreement with the known 0^+ state at 3.357 MeV; however, it is generally accepted (and is likely the case) that this state is far more complicated in its structure and that the two-particle two-hole "state" is likely found at around 7-MeV excitation. Thus it appears that phenomenological symmetry-energy parameters give agreement when compared with the experimentally observed states, but that the observed splittings actually arise from much more than just differences in symmetry energy.[30] This fact can have profound effects on all phenomenological approaches that try to fix the $T=0$ and $T=1$ particle-hole matrix elements solely on the basis of energy splittings. It should further be pointed out that the effect noted above is a general one; for example, the use of a similar procedure[28] places the lowest 0^+, $T=1$ state in ^{16}N degenerate with the ground state. It is at least 3.5 MeV above the ground state.

TABLE II. Overlap of $\langle {}^{42}\mathrm{Ca} \mid {}^{40}\mathrm{Ca} \rangle$ $T=1$ and $T=2$ 0^+ states.

Configuration	Transition	Amplitude
Final state	$(f_{7/2}{}^2)^0$ III	$(d_{3/2}{}^2)^0$ II
$T=1$	−0.217	+0.618
$T=2$	+0.120	+0.343

TABLE III. Overlap of $\langle^{42}\mathrm{Ca}|^{40}\mathrm{Ca}\rangle$ $T=0$ positive-parity states.

Final state	Configuration		Transition		Amplitude	
	$(f_{7/2}^2)^0$		$(p_{3/2}^2)^0$		$(d_{3/2}^2)^0$	
	I	III	I	III	II	IV
0_1^+	+0.742	+0.059	+0.163	+0.024	+0.130	+0.039
0_2^+	+0.166	−0.026	+0.026	−0.011	−0.057	−0.342
0_3^+	+0.310	−0.127	+0.068	−0.052	−0.279	+0.089
	$(f_{7/2}^2)^2$	$(p_{3/2}^2)^2$	$(f_{7/2}p_{3/2})^2$		$(d_{3/2}^2)^2$	
	III	III	III		II	IV
2_1^+	−0.044	−0.0167	−0.0494		+0.0642	+0.0356
2_2^+	−0.116	−0.044	−0.130		+0.166	−0.0135
		$(f_{7/2}^2)^4$	$(f_{7/2}p_{3/2})^4$			
4_1^+		0.0682	0.0608			
4_2^+		0.0223	0.0198			

Any shell-model calculation then will have great difficulties with the $T=0$, 0^+ states as the two-particle two-hole state will interact strongly with the four-particle four-hole state. Gerace and Green, eschewing any calculation of the unperturbed energies of these states, demand that the two-particle two-hole state be above the four-particle four-hole state.

For the DWBA calculations to the $T=1$, 0^+ state and the $T=2$, 0^+ state, the overlaps are calculated with the above expressions. As we assumed that these states are pure $(f_{7/2}^2 d_{3/2}^{-2})$, the $p_{3/2}$ components were removed from the ^{42}Ca ground state. The relative amplitudes of the two-particle and four-particle two-hole components, however, were kept fixed. Only transition II and transition III contribute (see Fig. 6) as the $T=1$ and $T=2$ states are pure two-particle two-hole.

SPECTROSCOPIC AMPLITUDES

The spectroscopic amplitudes obtained by projecting the final state of ^{40}Ca into the ^{42}Ca ground state are given in Tables II–IV. As each configuration contributes differently and coherently to the cross section, no spectroscopic factor can be defined. Even so, some estimate of the effects of coherence on the relative excitation of states of the same spin and parity can be made from an examination of the spectroscopic amplitudes if we assume that only the nuclear exterior contributes (the region in which the form factor has reached its asymptotic form.) From the amplitudes in Table II, the form factor for $f_{7/2}^2$ interfere constructively with the form factor for $d_{3/2}^2$ in the nuclear exterior for the $T=2$ state, but these form factors interfere destructively for the $T=1$ state. It appears that the coherence of two-nucleon transfer is constructive for the $T=2$ state, and destructive for the $T=1$ state. Presumably, it is by their difference that the $T=1$ state is suppressed relative to the $T=2$ state.

TABLE IV. Glendenning expansion for the overlap of $\langle^{42}\mathrm{Ca}|^{40}\mathrm{Ca}\rangle$ negative-parity states.

State	$n=2$	$n=1$
3^- $T=0$ 3.74	+0.080 82	−0.011 52
3^- $T=1$ 7.69	+0.006 01	−0.004 65
$3^- f_{7/2}^2 \rightarrow f_{7/2} d_{3/2}^{-1}$	+0.042 10	+0.008 16
5^- $T=0$ 4.92		+0.158
5^- $T=1$ 8.54		+0.123
$5^- f_{7/2}^2 \rightarrow f_{7/2} d_{3/2}^{-1}$		+0.175

For the $T=0$, 0^+ states in Table III, the contributions to the form factor for the ground state are all constructive in the nuclear exterior, but for the two excited states there are many cancellations. It is expected that the ground-state transition will be stronger than the transition to the excited states. For the 2^+ states, it should be noted that the form factors are roughly proportional to each other. As the form factors are proportional, it is safe to argue that the cross section to the higher 2^+ state should be a factor of 10 greater than the cross section to the lower 2^+ state. As the Q values for the two states are not so different, this expectation is quite independent of the DWBA calculation.

For the transitions to the negative-parity states, so many configurations contribute that it is not very illuminating to inspect the overlaps. Glendenning has given a harmonic-oscillator approximation to the form factor[31] which allows the dependence on the j_1 and j_2 to be evaluated. These coefficients were used to assess the amount of overlap (they were not used in the DWBA calcula-

tions), and the expansions are given in Table IV. The expansions appropriate for $(f_{7/2}^2) \rightarrow (f_{7/2}d_{3/2}^{-1})$ are also given, as $(f_{7/2}d_{3/2}^{-1})$ is the dominant component in the lowest $T=0$ and $T=1, 3^-$ and 5^- states. For the 7.69 – MeV, $T=1, 3^-$ state and the 3.73 – MeV, $T=0, 3^-$ state, as the form factors are proportional, it is reasonable to expect a cross section to the $T=1$ state of the order of one-hundredth of the cross section of the $T=0$ state. For the 5^- states, a cross section to the $T=1$ state of the order of half the cross section of the $T=0$ state is expected.

DWBA CALCULATIONS

The DWBA calculations for the two-nucleon transfer were performed with the code DWUCK2 in the local, zero-range approximation. It should be recalled that the striking feature of the data is the similarity of the $L=0$ angular distributions over a broad range of Q values. Five different states for which the spectroscopic amplitudes must differ widely, show maxima and minima at the same angles. It is reasonable then to demand of any parameter set that it produce $L=0$ angular distributions over a broad range of Q values and with pure configurations. Following previous (p, t) work at 40 MeV,[32] we chose the triton parameters of Hafele, Flynn, and Blair.[33] Proton parameters were taken from the work of Blumberg *et al.*[34] These optical-model parameters (with several other sets that are described below) are listed in Table V.

It was found that these parameters did reproduce reasonable $L=0$ angular distributions over a wide range of Q values, although the third maxima was somewhat too weak. For example, angular distributions for $(f_{7/2}^2)^0$, $(p_{3/2}^2)^0$, and $(d_{3/2}^2)^0$ for $Q=-11.35$ MeV, the ground-state transition, are shown in Fig. 8. As the parameter set adequately reproduced the stability of the $L=0$ angular distribution, it was applied to the configuration admixed form factors.

TABLE V. DWBA potentials. All potentials are of the form $1/\{1+\exp[(r-R)/a]\}$, where $R=r_0A^{1/3}$.

Reference	V	r	a	w	r'	a'
			Proton potential			
Blumberg	−43.3	1.18	0.700	−2.0	1.3	0.600
	Surface absorption of 5.0 MeV is included. Thomas form of spin-orbit potential of 6.0 MeV is included. Uniform charge distribution Coulomb potential included, $r_c=1.18$ fm.					
			Triton potentials			
Hafele	−146	1.24	0.678	−25.1	1.45	0.841
Chang	−136	1.10	0.654	−11.8	1.72	0.726
Glover	−135	1.40	0.600	−35	1.40	0.600
Flynn	−173	1.16	0.700	−14.8	1.65	0.806
Hiebert	−176	1.16	0.654	−10.0	1.64	0.910
	Uniform charge distribution Coulomb potential included, for Hafele, $r_c=1.24$ fm.					
			Bound state potential			
	V [a]	r	a			
		1.24	0.650			
	Thomas form of spin-orbit potential with $\lambda=25$ is included. Uniform charge distribution Coulomb potential included, $r_c=1.25$ fm.					

[a] Well depth is adjusted to produce bound state at one-half the two-nucleon separation energy.

A. Calculation of the ^{42}Ca$(p, t)^{40}$Ca $T=1$ and $T=2, 0^+$ states

Despite the fact that adequate angular distributions were produced for pure configurations, a consistent difficulty occurred for the configuration-admixed form factors. The angular distribution

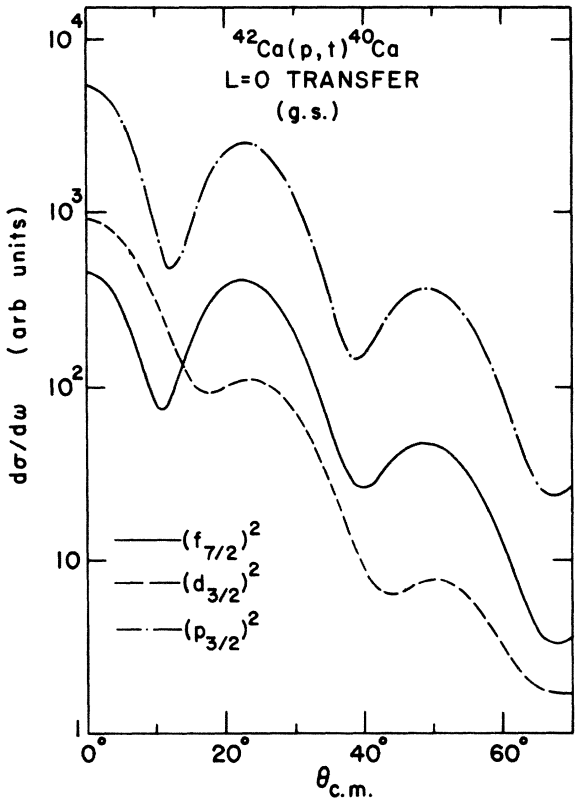

FIG. 8. DWBA calculation for $L=0$ transfer of $f_{7/2}^2$, $p_{3/2}^2$, and $d_{3/2}^2$ with $Q=-11.35$ MeV.

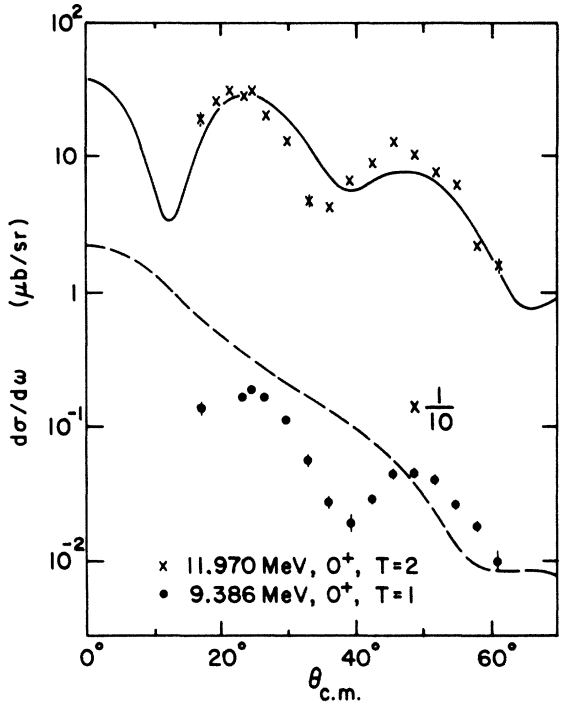

FIG. 9. DWBA calculations for $T=2$ and $T=1$, 0^+ states compared to the experimental data. The destructive interference of $f_{7/2}{}^2$ and $d_{3/2}{}^2$ results in a featureless angular distribution for the $T=1$ state.

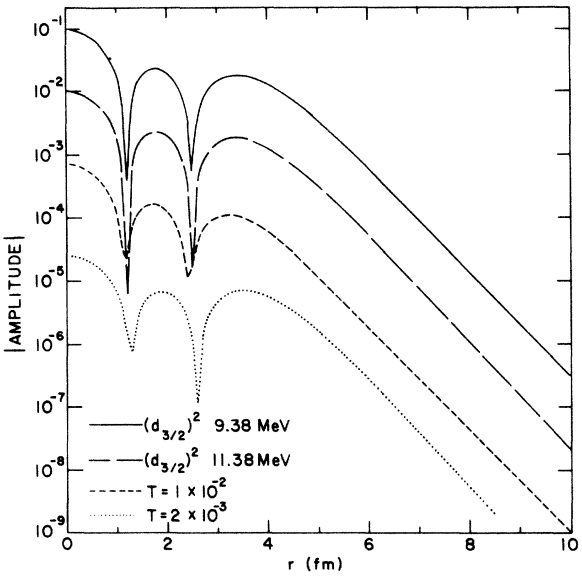

FIG. 10. Form factors for pickup to the ^{40}Ca $T=1$ and $T=2$, 0^+ states with spectroscopic amplitudes as given in Table II compared to pure $(d_{3/2}{}^2)^0$. Note that small changes in the interior cause large differences in the shape of the calculated angular distributions.

for the $T=2$, 0^+ state and the $T=1$, 0^+ state, along with the experimental data, are displayed in Fig. 9. The DWBA calculations are arbitrarily normalized to the 0^+, $T=2$ state. Although the calculated angular distribution to the $T=2$, 0^+ state is only moderately successful in reproducing the data, the calculated angular distribution for the $T=1$, 0^+ state is totally structureless. This destruction of the $T=1$, 0^+ angular distribution cannot be attributed to the difference in Q values, since the pure $(d_{3/2}{}^2)^0$ configuration at the appropriate Q values produced similar angular distributions.

The difference in the two form factors is due to the relative sign between $(f_{7/2}{}^2)^0$ and $(d_{3/2}{}^2)^0$. The form factors for the two states as calculated by the program DWUCK2 are shown in Fig. 10. [The form factors for the pure configuration $(d_{3/2}{}^2)^0$ at the appropriate Q values with unit spectroscopic amplitudes are shown for comparison.] They are remarkably similar; close inspection reveals that the nodes of the $T=1$ form factor are pulled in by 0.15 fm with respect to the $T=2$ form factor, and the third maximum of the $T=1$ form factor is reduced with respect to the third maximum of the $T=2$ form factor. These small changes can effect the angular distribution significantly only if this region of configuration space contributes to the radial integrals over the distorted waves.

The magnitude of the cross section also indicates that the nuclear interior is contributing to the DWBA. Although admixing $(f_{7/2}{}^2)^0$ constructively for the $T=2$ state increases the calculated cross

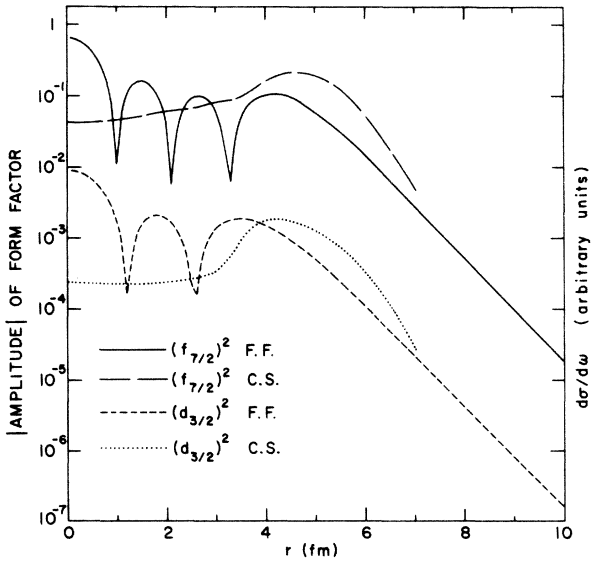

FIG. 11. DWBA cross section integrated from 10° to 60° calculated with radial cutoffs. The form factors are superimposed to illustrate the sensitivity of the DWBA calculation to the form factor in the interior.

section over pure $(d_{3/2}{}^2)^0$ by a factor of 3, admixing $(f_{7/2}{}^2)^0$ destructively for the $T=1$ state also increased the calculated cross section by 40%. Considering the magnitude of the cross section as a radial cutoff is applied is further evidence that the interior contributes. The magnitude of the integrated cross section calculated with different lower cutoffs is shown in Fig. 11. There is also displayed for comparison the pure $(f_{7/2}{}^2)^0$ and $(d_{3/2}{}^2)^0$ form factors. The sudden rise in cross section as the cutoff is increased from 3.0 fm to 4.5 fm shows that the interior is contributing to the integral. Since both the form factor and the distorted waves are highly oscillatory in the interior, it is not inconceivable that small changes in the form factor due to configuration mixing could cause changes in the cross section.

It was not possible to remove these difficulties by changing the triton optical-model potential. Two potentials with a real well depth of 176 MeV,[35,36] and two potentials with a real well depth of 130 MeV[37,38] (see Table V) were not able to produce $L=0$ angular distributions for both the $T=2$ and the $T=1$ form factors. These choices of triton potentials do not exhaust the available literature, but their range in parameter space adequately spans what has been currently proposed. Although it is not certain that this difficulty could not be removed by a different choice of optical potential, all potentials share two features. The protons are not strongly absorbed and enter the nuclear interior. The tritons are strongly absorbed, but not so strongly absorbed to suppress the near interior where the form factors differ.

B. Calculation of the ^{42}Ca$(p,t)^{40}$Ca positive-parity states

These difficulties in the superposition of $(d_{3/2}{}^2)^0$ and $(f_{7/2}{}^2)^0$ persist for the $T=0$, 0^+ angular distributions. The angular distributions for the three $T=0$, 0^+ states listed in Table III are displayed in Fig. 12. The standard proton, triton, and bound-state parameters are used. The experimental data are also displayed with the DWBA arbitrarily normalized to the 0_1^+ state. The structureless angular distributions for the excited states are the result of the inability to treat the destructive interference of $(d_{3/2}{}^2)^0$ and $(p_{3/2}{}^2)^0$ or $(f_{7/2}{}^2)^0$ properly.

Two not-unreasonable methods were found that produced $L=0$ angular distributions for all three

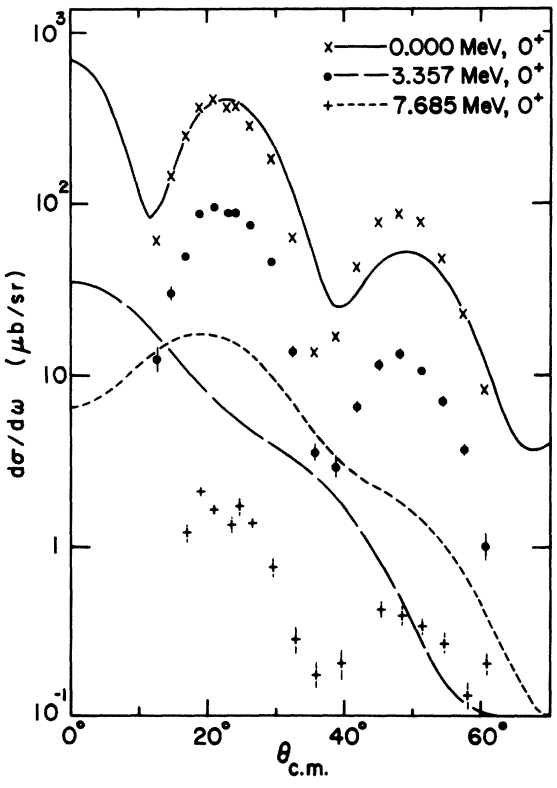

FIG. 12. DWBA calculations for $T=0$, 0^+ states compared to the experimental data. The destructive interference of $(fp)^2$ and $d_{3/2}{}^2$ results in featureless angular distributions for the 3.35- and 7.69-MeV states.

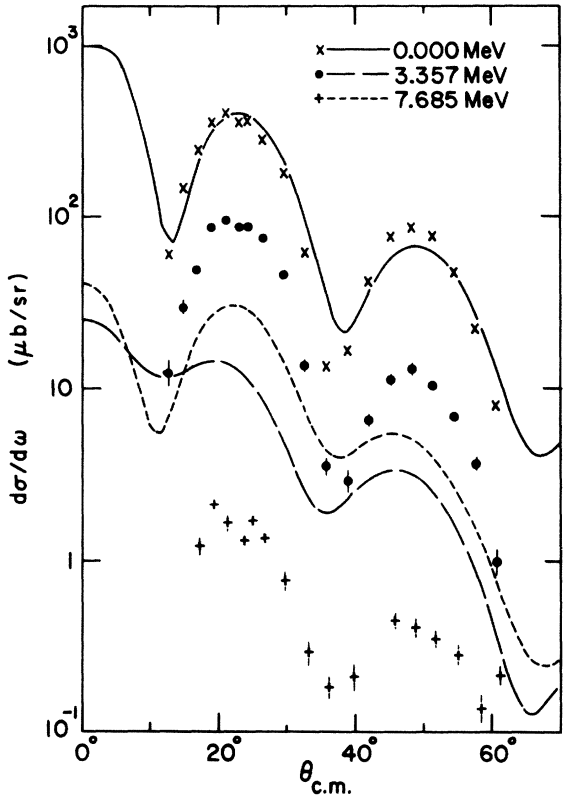

FIG. 13. DWBA calculations for $T=0$, 0^+ states compared to the experimental data. Particles are bound at the single-particle energy rather than the conventional separation energy.

TABLE VI. Comparison of integrated cross sections. Experimental and calculated cross sections are integrated over the angular range of 10°–60°.

State	Separation energy [c]	No $(d_{3/2}^2)^0$ [a]	Single-particle energy [d]	Experiment [b]
0_1^+ (0.00)	0.709×10^{-4} (100)	0.588×10^{-4} (100)	0.610×10^{-4} (100)	322. (100)
0_2^+ (3.35)	0.190×10^{-5} (2.7)	0.225×10^{-5} (4.3)	0.254×10^{-5} (4.1)	68.5 (20.6)
0_3^+ (7.68)	0.362×10^{-5} (5.1)	0.412×10^{-5} (7.0)	0.486×10^{-5} (8.0)	15.3 (4.8)
2_1^+ (3.90)	0.332×10^{-5} (4.67)			34.3 (10.7)
2_2^+ (6.91)	0.326×10^{-4} (45.8)			11.7 (3.63)

[a] Configuration-mixed form factor with all particles bound at one-half the two-nucleon separation energy, but without $d_{3/2}^2$ particles.

[b] Experimental cross section is in microbarns.

[c] Configuration-mixed form factor with all particles bound at one-half the two-nucleon separation energy.

[d] Configuration-mixed form factor with each particle bound at its single-particle energy.

states. Both methods succeed by suppressing the $(d_{3/2}^2)^0$ component in the form factor. Following Jaffee and Gerace[39] each nucleon was bound at the observed single-particle energy rather than one-half the two-neutron separation energy. As the single-particle energies for $d_{3/2}$, $f_{7/2}$, and $p_{3/2}$ are −15.7, −8.4, and −6.3 MeV, respectively, this procedure greatly reduces the contribution of the $(d_{3/2}^2)^0$ configuration. The angular distributions calculated for the 0_1^+, 0_2^+, and 0_3^+ states with the single-particle energy prescription are shown in Fig. 13. The DWBA calculations are arbitrarily normalized to the 0_1^+ state. When the $(d_{3/2}^2)^0$ was neglected completely, $L=0$ angular distributions again were produced.

The integrated cross sections that result from these procedures are compared to the data in Table VI. The three methods of calculation agree with one another within the accuracy of the two-nucleon transfer theory. As the three methods agree, there can be some confidence that a proper calculation would not produce grossly different cross sections. It should be noted that the calculated cross section for the first excited 0^+ state is too small by a factor of 5, while the calculated cross section of the second excited 0^+ state is about 40% too large. The DWBA calculations, using the spectroscopic amplitudes from the Gerace and Green wave functions, predict more strength to the two-particle two-hole state at 7.68 MeV than to the four-particle four-hole state at 3.35 MeV. This result is not unreasonable. Starting from an initial state which is predominantly two particle, it is expected that a final state of two-particle two-hole should be excited more strongly than a state of four-particle four-hole, which results from the smaller four-particle two-hole admixture in the initial state.

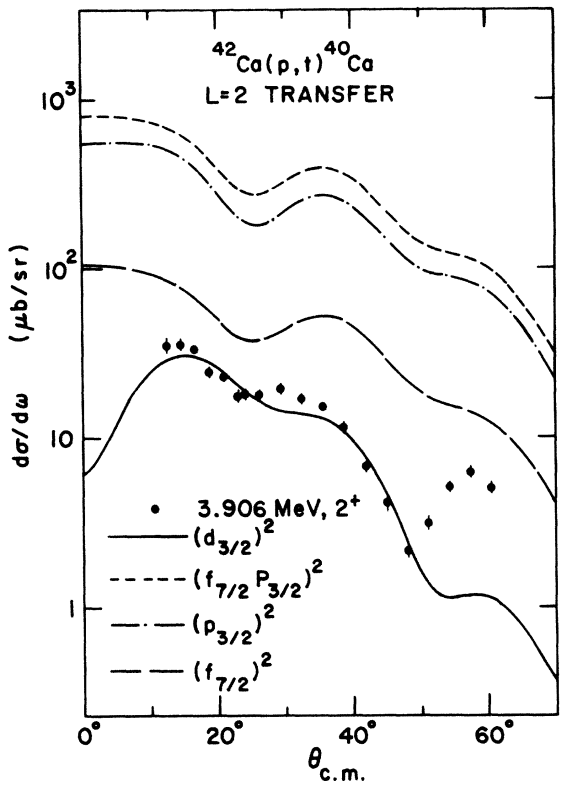

FIG. 14. DWBA calculation for $L=2$ transfer of $f_{7/2}^2$, $p_{3/2}^2$, $f_{7/2}p_{3/2}$, and $d_{3/2}^2$ with $Q=-15.25$.

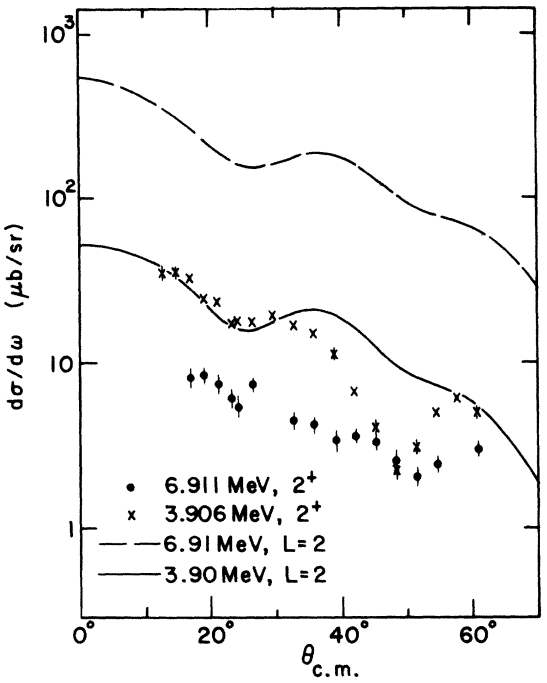

FIG. 15. DWBA calculations for 2^+ states compared to the experimental data. The calculation predicts more strength to the 6.90-MeV state than to the 3.90-MeV state. The data show less strength.

The same result was obtained for the $L=2$ transitions. The angular distributions for $(d_{3/2}{}^2)^2$, $(f_{7/2}{}^2)^2$, $(p_{3/2}{}^2)^2$, and $(f_{7/2}p_{3/2})^2$ are displayed in Fig. 14. The experimental data for the 3.907-MeV state are displayed for comparison. The angular distribution for $(d_{3/2}{}^2)^2$ produces an acceptable fit to the data, but the angular distributions for the other configurations are very different. The spectroscopic amplitudes for the 3.907-MeV state and the 6.911-MeV state are listed in Table III. The angular distributions for these two states are shown in Fig. 15. The data are displayed for comparison. The DWBA calculations are arbitrarily normalized to the 3.906-MeV state. The calculated angular distributions can be understood as the spectroscopic amplitudes are predominantly a superposition of $(f_{7/2}{}^2)^2$, $(p_{3/2}{}^2)^2$, and $(f_{7/2}p_{3/2})^2$, since the $(d_{3/2})^2$ component is kinematically suppressed. Ignoring the poor fit to the data, it should be noted that greater calculated strength is to the two-particle two-hole state at 6.911 MeV. The calculated strength to the 3.907-MeV state, which is predominantly four-particle four-hole, is smaller by a factor of 10. This situation is entirely analogous to the $L=0$ transition. The data show the greater strength in the lower state at 3.907 MeV, not the higher state at 6.911 MeV. The data are

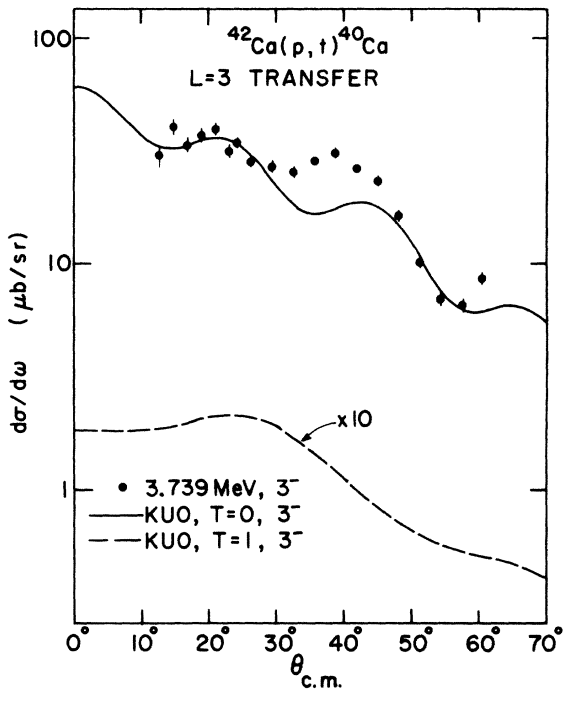

FIG. 16. DWBA calculations for 3^- states compared to the experimental data. Note the small predicted strength to the $T=1$, 3^- state.

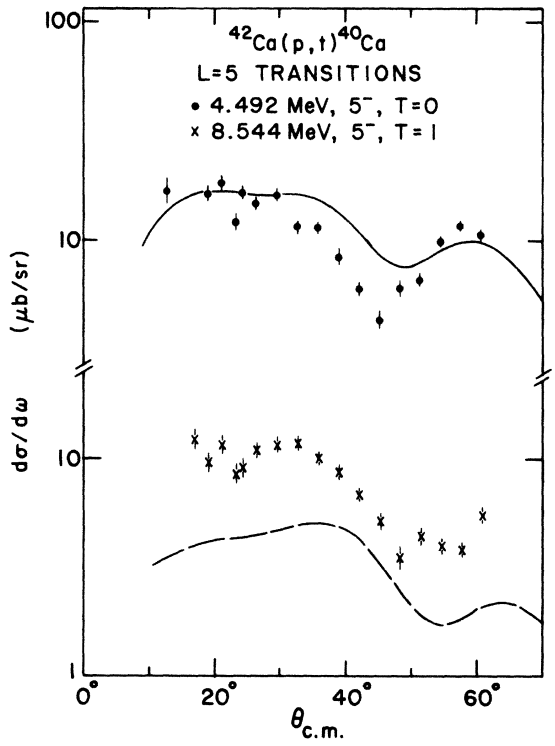

FIG. 17. DWBA calculations for 5^- states compared to the experimental data.

completely opposite from the calculations. These results are summarized in Table VI.

C. Calculation of the negative-parity states

No difficulties in the superposition of different configurations occurred in the calculation of the negative-parity states. The form factor for each configuration for the $L=3$ transition has one node, and the form factor for each configuration for the $L=5$ transition has no nodes. The angular distribution for the $T=0$, 3^- state is displayed in Fig. 16. The $T=0$ state is enhanced by a factor of 4 relative to the transition $(f_{7/2}{}^2)^0 \rightarrow (f_{7/2}d_{3/2}{}^{-1})^3$; the $T=1$ state is suppressed by a factor of 25 relative to the transition $(f_{7/2}{}^2)^0 \rightarrow (f_{7/2}d_{3/2}{}^{-1})^3$. Because of this extreme suppression of the $T=1$ state, the state does not appear in the spectrum. An examination of the spectroscopic amplitudes reveals how the suppression is so severe. All the transitions admixed to $f_{7/2}{}^2 \rightarrow f_{7/2}d_{3/2}{}^{-1}$ interfere constructively for the $T=0$ state, but those transitions interfere destructively for the $T=1$ state. Bertsch[40] has explained this effect in terms of correlations introduced by the residual particle-hole interaction.

For the $L=5$ transitions the calculated suppression of the $T=1$ state relative to the $T=0$ state is not as strong. The angular distributions for the 4.492-MeV $T=0$, 5^- state and the 8.544-MeV, $T=1$, 5^- state are displayed in Fig. 17. The $T=0$ state is enhanced by a factor of 1.28 over the $(f_{7/2}{}^2)^0 \rightarrow (f_{7/2}d_{3/2}{}^{-1})^5$, and the $T=1$ state is suppressed by a factor of 0.90 from the $(f_{7/2}{}^2)^0 \rightarrow (f_{7/2}d_{3/2}{}^{-1})^5$. The enhancement and suppression are weaker for the $L=5$ transitions as the spectroscopic amplitude for $(f_{7/2}d_{3/2}{}^{-1})$ dominates. There are fewer transitions than can interfere with $(f_{7/2}{}^2)^0 \rightarrow (f_{7/2}d_{3/2}{}^{-1})^L$ for $L=5$ than for $L=3$. Although the $T=1$ state is still calculated to be too weak, the disagreement is not serious.

CONCLUSIONS

The two-nucleon transfer reaction ^{42}Ca(p, t)^{40}Ca has been performed at 41.7 MeV with good resolution over an angular range of 10 to 60°. Three points can be made from the analysis of the data. First, the $T=1$, 0^+ state has been conclusively identified with the experimental yield corresponding to 9.386 ± 0.012 MeV excitation in ^{40}Ca. An explanation of the excitation of this state relative to the $T=2$, 0^+ state at 11.970 ± 0.012 MeV has been sought in terms of the interference from $f_{7/2}{}^2$ pickup, due to the four-particle two-hole component of ^{42}Ca, with the $d_{3/2}{}^2$ pickup from the two-particle part of ^{42}Ca. It was discovered that using the conventional two-nucleon transfer theory with reasonable optical-model parameters, it was not possible to reproduce the angular distribution to the $T=1$ state. In general, it was found that destructive interference of $(fp)^{2\ J=0}$ and $(sd)^{2\ J=0}$ produced structureless angular distributions. The calculational cause of this difficulty was traced to extreme sensitivity to the details of the form factor. A better calculation of these cross sections is needed to verify quantitatively the interference effect. It would also be advantageous to test the tacit assumption that the $T=2$ and $T=1$, 0^+ states are well described by the two-particle two-hole configurations chosen above.

Secondly, the proposed candidate for the $T=0$, 0^+ two-particle two-hole state at 7.30 MeV was found to be very weakly excited. An upper limit on the excitation of the 7.30-MeV state can be placed at 0.5 μb/sr, or 1% of the ground-state strength. Another candidate for the $T=0$, 0^+ two-particle two-hole state is the state found at 7.685 MeV. A careful inspection of all other experimental lines revealed no other line with an $L=0$ angular distribution in the region of excitation from 7.0 to 9.6 MeV.

Thirdly, the cross sections for the excitation of nine states treated by Gerace and Green were calculated with the DWBA code DWUCK2. The standard procedures for the distorted waves, and the form factor were respected. The spectroscopic amplitudes were derived from the wave functions of Gerace and Green. The inability to treat destructive interference of $(fp)^{2\ J=0}$ pickup and $(d_{3/2}{}^2)^{J=0}$ pickup caused structureless angular distributions for the 0_2^+ and 0_3^+. Two *ad hoc* procedures, which served to suppress the $(d_{3/2}{}^2)^{J=0}$ pickup, resulted in more reasonable angular distributions without changing the magnitude of the cross sections of these states significantly. The calculated strengths to the 3.35-MeV state and the 7.68-MeV state are, respectively, 4 and 7% of the ground-state strength. Previous two-nucleon transfer studies suggests that relative cross sections should be good to a factor of 2. The experimental result that the yields relative to the ground state of the 3.35-MeV state and the 7.68-MeV state are 21 and 4.8%, respectively, is well beyond the established uncertainties in the calculation.

A similar result was found to hold for the 2^+ states. The calculated cross section of the 3.90-MeV state is 4.7% of the ground-state strength; for the 6.91-MeV state it is 46% of the ground-state strength. The experimental result that the yield of the 3.90-MeV state is larger than the 6.91-MeV state (34.3 μb as compared with 11.7 μb) is opposite from the calculation. In both cases, the 0^+ states and the 2^+ states, experiment finds the greater strength to the state classified a four-particle four-hole, while the calculation finds the

greater strength to the state classified as two-particle two-hole. For the 2^+ states the calculated ratio is relatively independent of the DWBA calculation as the form factors are proportional.

The comparison between the experimental data and the DWBA calculations for the $T=0$ and $T=1$, 3^- and 5^- states is qualitatively correct. Configuration mixing suppresses the $T=1$, 3^- state relative to the $T=0$, 3^- state, but for the 5^- states, where configuration mixing is small, the suppression of the $T=1$ state, relative to the $T=0$ state, is also small.

The problem of the relative excitation of the positive-parity states is quite puzzling. The disagreement between the experiment and the calculation is greater than the suggested accuracy of the conventional two-nucleon transfer theory. Not only is the calculated strength to the four-particle four-hole, 0^+ and 2^+ states too small, but the calculated strength to the two-particle two-hole, 0^+ and 2^+ states is too large. To dispose of this latter difficulty, it has been suggested that the strength to the two-particle two-hole deformed states is actually shared by several states. However, significant fragmentation does not appear likely as all other 0^+ and 2^+ states were found to be very weakly excited.

It has also been suggested that including the $s_{1/2}$ orbital in the deformed state would change the calculation of the two-nucleon transfer cross section significantly. While a recent calculation[41] indicates that this possibility should be investigated, the conventional two-nucleon transfer calculation cannot substantiate this claim. The uncertainty introduced into the calculation by the binding energy prescription makes the inclusion of the $s_{1/2}$ orbital, which is much more tightly bound than the $d_{3/2}$ orbital, problematic.

Further work in the resolution of the questions raised above must be directed towards accounting for the electromagnetic data and the (p,t) data simultaneously. The impressive success of the Gerace and Green model in accounting for the electromagnetic decays must be a caution to any changes in their wave functions. The large yield to the four-particle four-hole state must also be viewed as a caution in the interpretation of multinucleon transfer reactions whose calculation is much more rudimentary than two-nucleon transfer. Although it appears unlikely that the coherent picture of ^{40}Ca that has developed can be abandoned, the possibility of a significant change in either the wave functions or the reaction calculation cannot be dismissed.

APPENDIX

The two-particle expansion is given in the text. The two-hole expansion is

$$|2\mathrm{h}K=0JM\rangle = p_J \sum_{j_3\geq j_4} \frac{1}{(1+\delta_{j_3 j_4})^{1/2}} (j_3\tfrac{3}{2} j_4 -\tfrac{3}{2}|J0)\chi(j_3\tfrac{3}{2})\chi(j_4-\tfrac{3}{2})|(j_3^{-1}j_4^{-1})^J\rangle$$

$$\equiv p_J \sum_{j_3\geq j_4} Y(j_3 j_4 J)|(j_3^{-1}j_4^{-1})^J\rangle,$$

where p_J normalizes the wave function and $Y(j_3 j_4 J)$ is introduced to compress the notation. The normalization factors n_J and p_J are

$$n_J^{-2} = \sum_{j_1\geq j_2} \frac{1}{1+\delta_{j_1 j_2}} |(j_1\tfrac{1}{2}\, j_2 -\tfrac{1}{2}|J0)|^2 |\chi(j_1\tfrac{1}{2})|^2 |\chi(j_2-\tfrac{1}{2})|^2 = \sum_{j_1\geq j_2} |V(j_1 j_2 J)|^2,$$

$$p_J^{-2} = \sum_{j_3\geq j_4} \frac{1}{1+\delta_{j_3 j_4}} |(j_3\tfrac{3}{2} j_4 -\tfrac{3}{2}|J0|^2 |\chi(j_3\tfrac{3}{2})|^2 |\chi(j_4-\tfrac{3}{2})|^2 = \sum_{j_3\geq j_4} |Y(j_3 j_4 J)|^2 .$$

For the two-particle two-hole state introduced in the text the normalization coefficient m_J is

$$m_J^{-2} = \sum_{J_\mathrm{p} J_\mathrm{h}} |(J_\mathrm{p} 0 J_\mathrm{h} 0|J0)|^2 n_{J_\mathrm{p}}^{-2} p_{J_\mathrm{h}}^{-2} .$$

Expressions for the four-particle two-hole state, the four-particle four-hole state, and their normaliza-

tion coefficients are given below:

$$|4\text{p2h}K=0JM\rangle = \sum l_J[X(j_1{}^\pi j_2{}^\pi j_3{}^\pi j_4{}^\pi J_p{}^\pi J^\pi J^\pi)V(j_7{}^\nu j_8{}^\nu J_p{}^\nu)(J^\pi 0 J_p{}^\nu 0|J0)$$

$$\times|\{[(j_1{}^\pi j_2{}^\pi)^{J_p{}^\pi}(j_3{}^{-1\,\pi} j_4{}^{-1\,\pi})^{J_h{}^\pi}]^{J^\pi}[(j_7{}^\nu j_8{}^\nu)^{J_p{}^\nu}\}^J\rangle$$

$$l_J{}^{-2} = \sum_{\substack{J_p{}^\pi J_h{}^\pi \\ J^\pi J_p{}^\nu}} n_{J_p{}^\pi}{}^{-2} p_{J_h{}^\pi}{}^{-2}|(J_p{}^\pi 0 J_h{}^\pi 0|J^\pi 0)|^2 n_{J_p{}^\nu}{}^{-2}|(J^\pi 0 J_p{}^\nu 0|J0)|^2$$

$$= \sum_{J^\pi J_p{}^\nu} m_{J^\pi}{}^{-2} n_{J^\nu}{}^{-2}|(J^\pi 0 J_p{}^\nu 0|J0)|^2,$$

$$|4\text{p4h}K=0JM\rangle = \sum k_J(J^\pi 0 J^\nu 0|J0)X(j_1{}^\pi j_2{}^\pi j_3{}^\pi j_4{}^\pi J_p{}^\pi J_h{}^\pi J^\pi)X(j_5{}^\nu j_6{}^\nu j_7{}^\nu j_8{}^\nu J_p{}^\nu J_h{}^\nu J^\nu)$$

$$\times|\{[(j_1{}^\pi j_2{}^\pi)^{J_p{}^\pi}(j_3{}^{-1\,\pi} j_4{}^{-1\,\pi})^{J_h{}^\pi}]^{J^\pi}[(j_5{}^\nu j_6{}^\nu)^{J_p{}^\nu}(j_7{}^{-1\,\nu} j_8{}^{-1\,\nu})^{J_h{}^\nu}]^{J^\nu}\}^J\rangle,$$

$$k_J{}^{-2} = \sum_{J^\pi J^\nu} m_{J_\pi}{}^{-2} m_{J_\nu}{}^{-2}|(J^\pi 0 J^\nu 0|J0)|^2.$$

Expression for $\langle(2\text{p2h})|\theta|(2\text{p})\rangle$ is given in the text. The three other routes are given below:

$$\text{I}\quad \langle 0\text{p0h})|\theta^{[j_A j_B]J}|(2\text{p})\rangle = \delta_{J0}\sum_{j_1} b_{j_1} F^{j_1 j_2 0}(R),$$

$$\text{III}\quad \langle(2\text{p2h})^{J_f}|\theta^{[j_A j_B]J}|(4\text{p2h})^0\rangle = \sum \frac{1}{\sqrt{3}} l_0 m_{J_f}|X(j_3 j_4 j_5 j_6 J_p J_h J_f|^2 V(j_7{}^\nu j_8{}^\nu J_f)F^{j_7{}^\nu j_8{}^\nu J_f}(R)$$

$$= \sum \frac{1}{\sqrt{3}}\frac{l_0}{m_{J_f}}\frac{1}{(2J_f+1)^{1/2}} V(j_7{}^\nu j_8{}^\nu J_f)F^{j_7{}^\nu j_8{}^\nu J_f}(R),$$

$$\text{IV}\quad \langle(4\text{p4h})^{J_f}|\theta^{[j_A j_B]J}|(4\text{p2h})^0\rangle = \sum_{\substack{J^{\nu'} J_p{}^\nu \\ j_9{}^{\nu'} j_{10}{}^{\nu'}}} \frac{k_{J_f} l_0}{m_{J_p{}^{\nu 2}} n_{J_p{}^{\nu 2}}}\frac{(2J^{\nu'}+1)}{(2J_p{}^\nu+1)(2J_f+1)}$$

$$\times|(J_p{}^\nu 0 J^{\nu'} 0|J_f 0)|^2 Y(j_9{}^{\nu'} j_{10}{}^{\nu'} J_f)F^{j_9{}^{\nu'} j_{10}{}^{\nu'} J_f}(R).$$

---

†Work supported in part by the U. S. Atomic Energy Commission, the National Science Foundation, and the Higgins Scientific Trust Fund.

*Present address: Physics Division, Argonne National Laboratory, Argonne, Illinois 60439.

[1]J. R. MacDonald, D. H. Wilkinson, and D. E. Alburger, Phys. Rev. C 3, 219 (1971).
[2]W. J. Gerace and A. M. Green, Nucl. Phys. A93, 110 (1967).
[3]W. J. Gerace and A. M. Green, Nucl. Phys. A113, 641 (1968).
[4]W. J. Gerace and A. M. Green, Nucl. Phys. A123, 241 (1968).
[5]P. Goode, Nucl. Phys. A140, 481 (1970).
[6]S. M. Smith and A. M. Berstein, Nucl. Phys. A125, 339 (1968).
[7]J. Cerny, R. H. Pehl, and G. T. Garvey, Phys. Lett. 12, 234 (1964).
[8]J. P. Schapira, M. Chabre, Y. Dupont, and P. Martin, Phys. Rev. C 5, 1593 (1972).
[9]E. G. Adelberger, P. T. Debevec, G. T. Garvey, and R. Ohanian, Phys. Rev. Lett. 29, 883 (1972).
[10]P. T. Debevec and G. T. Garvey, Bull. Am. Phys. Soc. 17, 91 (1972).
[11]I. S. Sherman and R. G. Roddick, IEEE Trans. Nucl. Sci. NS17, 252 (1970).
[12]J. R. Comfort, Argonne National Laboratory Physics Division Informal Report No. PHY-1970B, 1970 (unpub-

lished).
[13]A. N. James, P. R. Anderson, D. C. Bailey, P. E. Carr, J. L. Durell, M. W. Greene, and J. F. Sharpey-Schafer, Nucl. Phys. A172, 401 (1971).
[14]Ignoring Q dependence, for two-particle two-hole 0^+ states excited by creating two holes via pickup on the two-particle target, the ratio of $T=2:T=1:T=0$ final states is $1:3:2$ for ^{40}Ca, and the ratio $T=2:T=1$ is $1:1$ for ^{40}K.
[15]H. P. Leenhouts, Physica 35, 290 (1967).
[16]Although Schapira *et al.* (Ref. 8) and we previously identified this line as the $T=1$, 3^- state at 7.693 MeV, this assignment causes great difficulties; the observed cross section relative to the $T=0$, 3^- state at 3.737 MeV is much larger than the DWBA with reasonable wave functions will allow. The assignment of 0^+ was urged on us by Dr. K. K. Seth on the basis of his ^{42}Ca-$(p,t)^{40}$Ca work at the Michigan State University cyclotron. We are indebted to Dr. Seth for his correction of this misassignment in our previous work.
[17]P. Federman and S. Pittel, Phys. Rev. 186, 1106 (1969).
[18]I. S. Towner and J. C. Hardy, Advan. Phys. 18, 401 (1969).
[19]N. K. Glendenning, Phys. Rev. 156, 1344 (1967).
[20]S. Kahana and D. Kurath, Phys. Rev. C 3, 543 (1971).
[21]B. F. Bayman and A. Kallio, Phys. Rev. 156, 1121 (1967).
[22]P. D. Kunz, University of Colorado Report COO-535-606 (unpublished).
[23]T. T. S. Kuo, private communication. These wave functions are the Tamm-Dancoff approximation of Gerace and Green's Nucl. Phys. A114, 641 (1968), Table 14.
[24]A. de-Shalit and I. Talmi, *Nuclear Shell Theory* (Academic, New York, 1963).
[25]F. C. Erné, Nucl. Phys. 84, 91 (1966).
[26]A. Zuker, in *Proceedings of the Topical Conference on the Structure of $1f_{7/2}$ Nuclei, Padua, Italy, 1971*, edited by R. A. Ricci (Editrice Compositori, Bologna, 1971), p. 95.
[27]R. Bansal and J. B. French, Phys. Lett. 11, 145 (1964).
[28]L. Zamick, Phys. Lett. 19, 580 (1965).
[29]L. Zamick, Ann. Phys. (N.Y.) 77, 230 (1973).
[30]Realistic forces produce a much smaller symmetry energy. This symmetry energy does account for the splitting of the two-particle two-hole states but not the particle-hole states (Ref. 29).
[31]N. K. Glendenning, University of California Report No. UCRL-18268 (unpublished).
[32]B. F. Bayman and N. M. Hintz, Phys. Rev. 172, 1113 (1968).
[33]J. C. Hafele, E. R. Flynn, and A. G. Blair, Phys. Rev. 155, 1238 (1967).
[34]L. N. Blumberg, E. E. Gross, A. Van der Woude, A. Zucker, and R. H. Bassel, Phys. Rev. 147, 812 (1966).
[35]E. R. Flynn, D. D. Armstrong, J. G. Berry, and A. G. Blair, Phys. Rev. 182, 1113 (1969).
[36]J. C. Hiebert, E. Newman, and R. H. Bassel, Phys. Rev. 154, 898 (1971).
[37]H. H. Chang and B. W. Ridley, University of Colorado Technical Report No. COO-535-653, 1971 (unpublished).
[38]R. N. Glover and A. D. W. Jones, Nucl. Phys. 81, 265 (1966).
[39]R. L. Jaffee and W. J. Gerace, Nucl. Phys. A125, 1 (1969).
[40]G. F. Bertsch, *The Practitioner's Shell Model* (North-Holland, Amsterdam, 1972).
[41]T. Erikson, V. Horsfjord, and B. Nilsson, Phys. Lett. 46B, 173 (1973).